



# Profiling population-level diversity and dynamics of *Accumulibacter* via high throughput sequencing of *ppk1*

Wei Song<sup>1</sup> · Min Jia Zheng<sup>1</sup> · Hao Li<sup>1</sup> · Wei Zheng<sup>1</sup> · Feng Guo<sup>1</sup>

Received: 18 June 2019 / Revised: 9 September 2019 / Accepted: 7 October 2019 / Published online: 8 November 2019  
© Springer-Verlag GmbH Germany, part of Springer Nature 2019

## Abstract

As the key organism for enhanced biological phosphorus removal, *Accumulibacter* has shown high intragenus diversity based on the phylogeny of polyphosphate kinase I gene (*ppk1*) and many clade-specific features related to performance of wastewater treatment. However, the widely used molecular approaches are deficient or cost-inefficient in providing a comprehensive and quantitative population-level profile for *Accumulibacter* in complex community. In this study, we introduced a pipeline to analyze the population-level diversity and dynamics of *Accumulibacter* via high throughput sequencing (HTS) of *ppk1* and 16S rRNA gene simultaneously. The HTS approach was assessed by testing primer coverage, performing sample replication, and comparing with a traditional clone library. Based on survey on full-scale activated sludge samples, unexpected high microdiversity in *Accumulibacter* and a tendency of exclusivity between two phylogenetic types were discovered. Moreover, the pipeline facilitated monitoring the population-level dynamics and co-occurrence pattern under various laboratory enriching conditions. The results revealed previously uncharacterized intraclade dynamics during enrichment, little effect of denitrifying process on the *Accumulibacter* diversity, and the niche adaptation of Clade IIC on propionate as sole carbon source. Co-occurrence of *Accumulibacter* populations further partially supported the exclusivity of two types. A few bacterial taxa, including *Cytophagaceae*-, *Prostheco*-, and *Compeibacter*-related taxa, showed co-occurrence with many *Accumulibacter* populations, suggesting their niche co-selection or potential metabolic interactions with *Accumulibacter*. The present pipeline is transplantable for studying microdiversity and niche differentiation of other functional microorganisms in complex microbial systems.

**Keywords** Enhanced biological phosphate removal · Activated sludge · Microdiversity · Co-occurrence

## Introduction

Nutrient removal in wastewater is essential for environmental health. The process of enhanced biological phosphorus removal (EBPR) fundamentally relies on specialized microbial taxa with the metabolic behavior of excessive phosphate accumulation (Nancharaiyah et al. 2016; Oehmen et al. 2007; Slater et al. 2010). So far, the most well-studied polyphosphate-accumulating

organism (PAO) is *Candidatus Accumulibacter* (hereafter referred to as *Accumulibacter*), which has no cultured representatives within *Betaproteobacteria* (Barr et al. 2016; Garcia Martin et al. 2006; Oyserman et al. 2016; Skennerton et al. 2015). Considering the poor intragenus taxonomic resolution of the 16S rRNA gene, the functional gene of polyphosphate kinase I (*ppk1*) has been referred in phylogenetic analysis within the genus (He et al. 2007). Diverse clades belonging to two types have been classified in this genus with different niche differentiation features (Peterson et al. 2008). At present, 14 clades were assigned in *Accumulibacter*, with 5 and 9 clades belonging to types I and II, respectively (Mao et al. 2015). Continuous studies focused on the type- and clade-specific phenotypes and practical performance (e.g., suitability to oxygenic conditions, temperature, capability of denitrification, tolerance to phosphate concentration.) in full- and laboratory-scale EBPR systems are present (Albertsen et al. 2012; Camejo et al. 2016; Nurmiyanto et al. 2017; Ong et al. 2013; Saad et al. 2016; Welles et al. 2016).

**Electronic supplementary material** The online version of this article (<https://doi.org/10.1007/s00253-019-10183-9>) contains supplementary material, which is available to authorized users.

Wei Song and Min Jia Zheng are co-first authors.

✉ Feng Guo  
fguo.bio@xmu.edu.cn

<sup>1</sup> School of Life Science, Xiamen University, Fujian 361102, People's Republic of China

For example, a recent study provided the first integrated omics evidence that a strain from clade I-C is a denitrifier under microaerobic condition containing complete denitrification genes (Camejo et al. 2019). *ppk1* is also a single-copy gene in this genus (Garcia Martin et al. 2006; Skennerton et al. 2015), thereby supporting its suitability in quantifying multiple population abundances within the genus.

Researchers have applied many techniques to identify and quantify the type or clade-level population for environmental samples containing *Accumulibacter*. The construction of the clone library of the *ppk1* PCR amplicon generated from conserved primer set is the most widely used approach, by which typically dozens of colonies are randomly selected, and sequences are obtained for the overall population-level profile of one sample (Mao et al. 2015; Peterson et al. 2008). However, this method suffers from high cost, low throughput, and poor detectability when dealing with large sample sets and subdominant populations. The methods of restriction enzymatic digestion and clade-specific quantitative PCR are time efficient (Camejo et al. 2016; Slater et al. 2010; Zhang et al. 2016). However, they may be unreliable, because these methods generally cannot obtain the full image of all potential *Accumulibacter* clades in samples without preliminary knowledge. Unknown cross-talking and coverage for the clade-specific restriction enzymes and primers can introduce other biases. rRNA-based fluorescence in situ hybridization (FISH) is the exclusive solution to study the morphology and spatial distribution of *Accumulibacter* (Flowers et al. 2009; Li et al. 2019). However, it can hardly distinguish all clades because no precise and comprehensive linkage between 16S rRNA genes and *ppk1* sequences for most clades can be constructed. The false positive of the FISH technique on *Accumulibacter* determination has been observed due to the hybridization with phylogenetically close taxa (Albertsen et al. 2016). As a state-of-the-art approach, direct metagenomic sequencing has also provided valuable information to understand the genomic diversity of this genus (Skennerton et al. 2015). However, direct metagenomic sequencing also suffers from high cost and potential deficiencies in the presence of microdiversity (Albertsen et al. 2012).

As a cost-effective method for comparing the clone library, the high throughput sequencing (HTS) of the functional gene amplicon other than 16S rRNA genes has been used to profile many functional taxa, such as nitrogen cycling and methane oxidization groups in complex environmental samples (Kip et al. 2011; Remmas et al. 2016). In most cases, the targeted gene (e.g., denitrification genes) is not limited to a certain taxonomic lineage to obtain a comprehensive profile. However, a study profiling the nitrite oxidoreductase gene in the genus *Nitrospira* has shown an unexpectedly high intragenus heterogeneity within a single activated sludge (AS) sample (Gruber-Dorninger et al. 2015). This result indicated a previously ignored microdiversity for functional taxa

that co-occurred in the complex systems. In this study, we propose to test a pipeline in analyzing the population diversity and dynamics of *Accumulibacter* on the basis of HTS of 16S rRNA and *ppk1*. This pipeline can be used in the unambiguous determination of population-level diversity and dynamics of *Accumulibacter* and may serve as an example for studying the microdiversity and niche differentiation of the functional taxa in complex microbial systems.

## Materials and methods

### AS samples

In this study, AS samples were collected from full-scale WWTPs and laboratory EBPR bioreactors. AS samples (100 mL) from seven WWTPs in seven distantly separated cities in China (designated as YC, SY, PJ, HZ, CD, ZB, and XA) were fixed with 50% ethanol (final concentration, referred to Zhang et al. 2012) on site and stored at  $-20\text{ }^{\circ}\text{C}$  before DNA extraction (Table S1). Duplicate biomass for six AS samples (except for XA) were analyzed to examine the reproducibility for the analytic pipeline.

EBPR bioreactors were operated in laboratory under various conditions. One 3-L mother reactor (MR) was kept running, with a basic setting following the information on Vargas et al.'s (2009) study. Since April 2016, the approach was modified by using acetate and propionate (each having the same chemical O demand concentration) as the C source. Six samples within 730–797 days after the starting day were collected. Five 1-L reactors were inoculated from MR and kept running for approximately 5 weeks under various conditions, including continuous aeration (R1), control treatment (R2, essentially the same as MR),  $\text{NH}_3$  oxidization inhibition (R3), and the use of acetate (R4) and propionate (R5) as the sole C sources. To monitor the operational performance of the five bioreactors (R1–R5), we measured  $\text{PO}_4\text{-P}$ ,  $\text{NH}_3\text{-N}$ , and  $\text{NO}_3\text{-N}$  according to the standard methods (APHA 1998). Another 1-L reactor (designated as R') was inoculated with seed AS from a full-scale WWTP (located in Xiamen University, Xiamen; the XA sample was mentioned above). All the AS samples from the bioreactors were fixed with 50% ethanol and stored at  $-20\text{ }^{\circ}\text{C}$  before DNA extraction (see Figure S1 for the details on operational and sampling information).

### DNA extraction

DNA extraction was performed using the FastDNA SPIN kit for Soil (Mpbio, USA) following the manufacturer's instruction. The DNA quantity and quality were evaluated by the  $\text{OD}_{260}$  and  $\text{OD}_{260}/\text{OD}_{280}$  ratio with a microspectrophotometer (NanoDrop, ND-1000, Thermo Scientific, USA),

respectively. The OD<sub>260</sub>/OD<sub>280</sub> ratios of all DNA samples ranged from 1.7 to 1.9.

### Designing HTS primer set targeting on *Accumulibacter ppk1*

According to two previous studies (Mao et al. 2015; Peterson et al. 2008), 29 *ppk1* sequences representing the known 14 clades were obtained from the GenBank. The *ppk1* sequences from 13 available *Accumulibacter* genomes were added (Camejo et al. 2019; Garcia Martin et al. 2006; Mao et al. 2014; Skennerton et al. 2015). The *ppk1* sequences from *Rhodocyclus tenuis*, *Propionivibrio* sp., and *Dechloromonas agitata* (accession nos. AF502199, FLQY01, and JEAT01 in NCBI) were referred as the outgroup. Most of the available *ppk1* sequences of *Accumulibacter* were generated from the 254F and 1376R primer sets (He et al. 2007). Thus, only the suitable primer within the region can be effectively searched. A conserved reverse primer (526R: 5'-RTTGAGRCTCTTGT TGA-3') was designed. We used 254F and 526R to perform the PCR amplification of *ppk1* for *Accumulibacter*.

### PCR amplification of 16S rRNA gene from total bacteria and *ppk1* from *Accumulibacter*

The conditions of the PCR amplification for the V4 region of the bacterial 16S rRNA gene (V4F and V4R) and the long fragment of *Accumulibacter ppk1* (by using primers 254F and 1376R) were referred to the references (Kozich et al. 2013; Mao et al. 2015). For the short fragment of *ppk1*, the PCR condition was also referred to the V4 amplification with modified Tm at 50 °C. The 8 nt barcode and 2 nt linker sequence were added to the 5'-end of the primers for V4 (V4F-XXXXXXXXXGTGTGC CAGCMGCCGCGGTAA and V4R-XXXXXXXXXC<sup>U</sup>CGGAC TACHVGGGTWTCTAAT) and short fragment of *ppk1* (254F-XXXXXXXXXCTCACCACCGACGGCAAGAC and 526R-XXXXXXXXX<sup>U</sup>TRTTGAGRCTCTTGTGTA) in multiplying and minimizing the barcode-introduced PCR biases, respectively. We used unique dual barcodes for each sample to minimize cross-talking among samples (MacConaill et al. 2018). Any 8 nt barcode, regardless of the added forward or reverse primer, was only assigned to one sample within a sequencing library. The PCR products for each sample were purified and pooled with equal mass before library construction.

### HTS and data cleaning

After HTS library construction, the HTS for the amplicons of the 16S rRNA gene V4 region and *ppk1* were performed on the ILLUMINA HiSeq 2500 platform with PE250 strategy (commercial service of Novogene, Beijing, China). The raw sequencing data was prefiltered by requiring the average *Q* value of > 15 within any 4 nt window.

### Pipeline for analysis of population-level diversity of *Accumulibacter*

A diagram for the pipeline was elucidated in Figure S2. To profile the population-level diversity and community structure for *Accumulibacter*, we determined the zero-radius operational taxonomic units (zOtu, hereafter referred to as Otu) for V4 and *ppk1* amplicon by combining Mothur and USEARCH programs (Edgar 2010; Kozich et al. 2013). The pipeline was described as follows. For rRNA gene or *ppk1*, the paired-end reads were merged into tags and demultiplexed to certain sample according to the dual barcodes (default setting in Mothur). The combined file containing all primer-free tags was introduced to USEARCH to denoise the sequencing errors by using the UNOISE2 algorithm with default settings (Edgar 2016b). UCHIME2 algorithm was utilized to remove chimeras (Edgar 2016a). The zOtu tables were generated, and possible cross-talking was further cleaned by the UNCROSS2 algorithm in the USEARCH (Edgar 2018). Then, we performed data analysis for 16S rRNA gene and *ppk1* divergently to classify or annotate the zOtu representatives.

For the 16S rRNA gene, we classified all zOtu in the Mothur program (default setting via classify.seqs command) by referring to the EzBioCloud database, which consists of all strains and clustered molecular species containing *Accumulibacter* (Yoon et al. 2017). The nonbacterial sequences were removed from the zOtu table. Then, the sampling depth was normalized to 10,000 for each sample. The relative abundance of *Accumulibacter* in the total bacteria was calculated by adding the relative abundances of all Otu classified as *Accumulibacter*.

For the *ppk1* sequences, we extracted all zOtu sequences and performed BLASTN against a customized database of *ppk1* from *Accumulibacter* (BLASTN). The database contained 42 *ppk1* sequences from 14 *Accumulibacter* clades as mentioned above. A considerable number of the reference sequences did not contain the first 35 nucleotides after 254F. Thus, all references were trimmed accordingly, and the alignment length for a primer-free HTS amplicon sequence should be 201 nt against the references. Sequences passed through a threshold with > 190 nt alignment length (95% length of the primer-free amplicon), and 81% similarity to any reference was kept for downstream analysis. The similarity cut-off was determined according to an investigation of the intragenus similarity for *Accumulibacter ppk1*. Within the 254F–526R region of the 45 references (including the three out-groups), for any sequence from *Accumulibacter*, the closest similarity to another intragenus sequence was ≥ 81%, while it was < 79% in any outgroup. Then, the sampling depth was also normalized to 10,000 for each sample. Two relative abundances can be calculated based on the zOtu tables of *ppk1* and V4. One was the certain *Accumulibacter* population to total *Accumulibacter*, and the other was the certain

*Accumulibacter* population to total bacteria by referring to the relative abundance of all *Accumulibacter* to total bacteria.

### Comparison of HTS data and results from clone library

Two AS samples (i.e., YC and HZ) were chosen to compare the results from HTS and clone library. The construction of the clone libraries was performed in accordance with the study of Mao et al. (2015). To compare the HTS result with that of clone libraries, we first trimmed the 254F-526R primer-free fragments of the clone sequences and clustered into 0.995-level Otus, thereby allowing one different site. Representative sequences were selected and combined as the reference database. Then, each *ppk1* Otus from HTS was searched using BLASTN against the database and only hit with > 99.5% similarity. A 235 nt alignment length was maintained. The shared and unique sequences were determined, and their abundances were calculated for each method.

### Data analysis and visualization

Average nucleotide identity (ANI) calculation for *Accumulibacter* genome pairs was performed according to the MiSI method (Varghese et al. 2015).  $\alpha$ - and  $\beta$ -diversity analyses were performed in Mothur (Kozich et al. 2013). PCA analysis for V4 and *ppk1* data was visualized using the Phyloseq package following the pipeline of Microbiota Analysis in R (McMurdie and Holmes 2013; [https://rpubs.com/dillmcfarlan/R\\_microbiotaSOP](https://rpubs.com/dillmcfarlan/R_microbiotaSOP)). The construction of the phylogenetic tree and calculation of distances between sequences were realized in the MEGA 7.0 software (Kumar et al. 2016). Heatmap was drawn in R by using the *heatmap* package (<https://CRAN.R-project.org/package=heatmap>). Co-occurrence analysis was performed essentially according to Ju and Zhang (2015). Only correlations with Spearman coefficient were > 0.7 or  $\leq 0.7$  ( $P < 0.01$ ) was kept before visualization in the Gephi program (Bastian et al. 2009).

## Results

### Evaluation of primer 526R according to reference sequences

As shown in Fig. 1(a), primer 526R perfectly matched nearly all the 42 *ppk1* references from *Accumulibacter* except for EU432714. We downloaded 1,024 dereplicated *ppk1* sequences of *Accumulibacter* from NCBI nucleotide database, and > 94% of the *ppk1* sequences can perfectly match with the primer. Moreover, > 99% of them had no mismatch within the initial 8 nt of the 3' region (data not shown). Therefore, this primer theoretically can cover most of the known *Accumulibacter* populations. 526R can also perfectly match the *ppk1* from *R. tenuis*

and *Dechloromonas agitate*. However, the 3'-end mismatch of primer 254F determined the unavailability of the amplification to out-groups. According to the sequence comparison, *ppk1* from the well-known *Accumulibacter* can be specifically amplified using 254F and 526R.

Given that 13 *Accumulibacter* genomes with their *ppk1* are collected in the database, we also examined whether the distance of *ppk1* is related to the genomic divergence for any of the two *Accumulibacter* strains. As shown in Fig. 1(b), strong correlations were found between the similarities of both amplifying regions (254F-1376R and 254F-526R) and genomic ANI value and between the similarities of the two amplifying regions. The 254F-526R amplicon can generally represent the genomic divergence between *Accumulibacter* strains. Short 254F-526R amplicon exhibited higher divergences than long 254F-1376R amplicon because the distance of the former was 1.18-fold higher than that of the latter on average. The only intraspecies pair (LBIV01 vs. JDST02, ANI = 99.8%) had a detectable divergence between their *ppk1* sequences (~ 3%), thereby suggesting that the gene can have a taxonomic resolution below the species level at least in some cases.

### HTS profiling *Accumulibacter* diversity in AS from full-scale WWTPs

Figure 2(a) shows that according to the V4 data, all seven full-scale AS samples (with duplications) had relatively low *Accumulibacter* abundances in the total bacterial community. The percentages were > 1% only in two samples, namely XA and YC, whereas those of other samples varied from 0 to 0.37%. These abundances were close to the results of previous reports on non-EBPR full-scale AS samples (Mao et al. 2015). Sample CD-II had no *Accumulibacter* detected in the V4 data, whereas the *ppk1* amplification and sequencing succeeded. This result agreed that lineage-specific gene was more sensitive than the universal gene if the sequencing depth was the same. The detected number of *Accumulibacter* Otus for the V4 data was overall positively correlated with the number of *ppk1* Otus. However, the latter was generally 8- to 12-fold higher than the former, thereby indicating the low resolution of the V4 data. According to the *ppk1* data, 143 Otus was detected in all seven samples, each of which contained 6–78 *ppk1* Otus. All 14 clades had hits if all samples were combined together. The populations in 11 clades (except for I-D, I-E, and II-I) exhibited > 1% relative abundances at least in one sample (total *Accumulibacter*, according to *ppk1* data only).

Except for the CD sample, all DNA-level duplicates also exhibited high reproducibility, which validated the technical robustness of the pipeline (Figure S3). The variation in the CD sample should be attributed to the extremely low abundance of *Accumulibacter*, as revealed by the V4 data (Fig. 2(a)).

Although the most *ppk1* Otu sequences shared > 90% similarity to the database references, 16 of these sequences shared

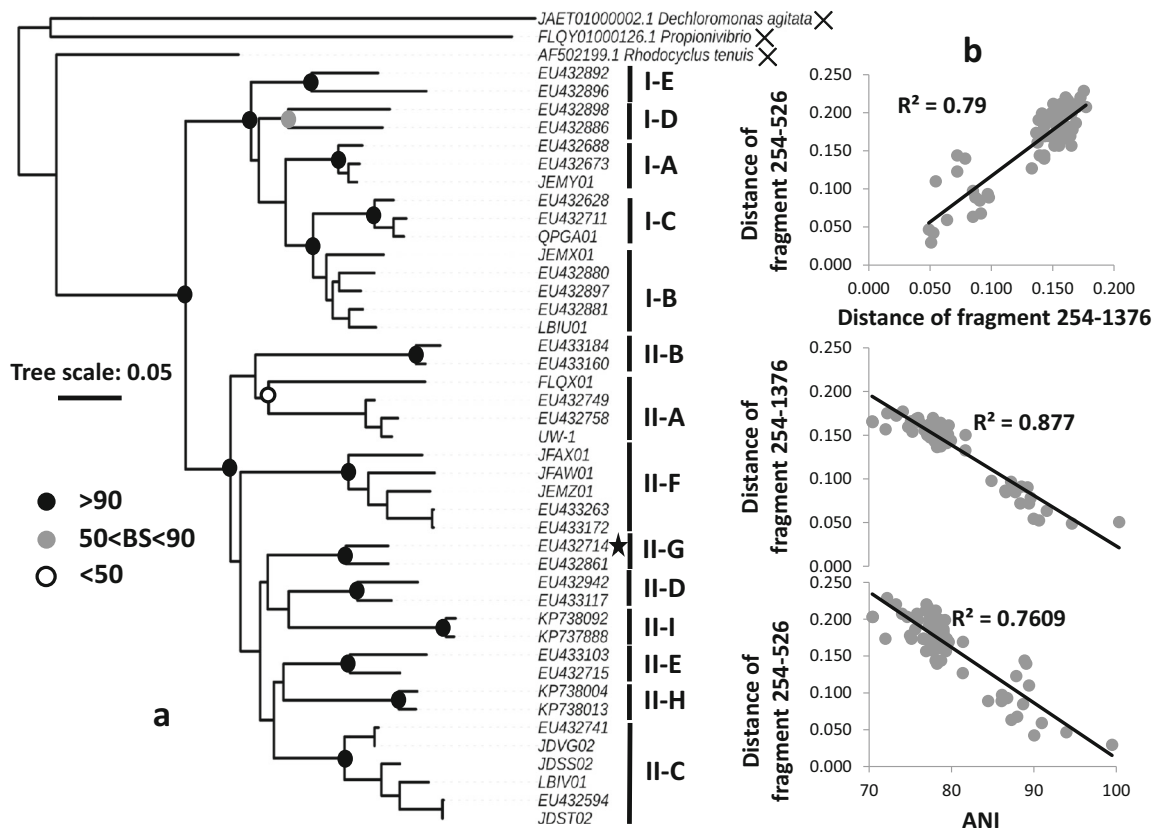


**Fig. 1** Phylogenetic tree of selected representatives from 14 *Accumulibacter* clades (a) and regression analysis of distances among *ppk1* sequences and ANI values for genomic pairs (b). The maximum likelihood tree was constructed using the TN92 + G + I model, which was

determined as the best model tested in MEGA 7.0. The data involved in the regressions were only for those *ppk1* sequences extracted from 13 genomes. The pairs with the ANI of < 70% were removed

< 90% similarity to any subject (Fig. 2(b)). The latter populations represented novel clades compared with the 14 known ones. For each sample, the sequences were also clustered based on their similarity. As shown in Fig. 2(c), the samples with zero-radius Otus also contained clustered ones. At the distance cut-off of 0.09, 5–17 Otus were still detected in each of the seven samples, thereby suggesting a conservation pool containing phylogenetically divergent *Accumulibacter* populations in each AS. We calculated the relative abundance of types I and II populations in each sample. A negative distribution pattern showed two types that were nearly exclusively dominant in all samples (Fig. 2(d)).

### Comparing HTS and clone library results

Two AS samples, namely HZ and YC, with relatively high *Accumulibacter* population-level diversity, were determined by HTS profiling and selected for clone library construction. For 62 clone sequences (31 each from HZ and YC), only three clone sequences had mismatches with the 526R primer, and the mismatches were all located in the middle or 5'-region of the primer. All the three clone sequences can be found in the HTS dataset, thereby indicating PCR's potential fault tolerance. Ten and

thirteen clone representatives (dereplicate similar sequences with > 99.8% similarity) were compared with HTS Otus for HZ and YC, respectively. All clones except for HZ19 and YC35 were detected in the HTS data. Further examination proved that YC35 was found in the original HTS data but subsequently removed in the pipeline due to its extremely low abundance (0.01% in the original data). Comparing the HTS quantification results with that of the clone libraries showed that they were overall comparable for most populations, especially the dominant ones (Fig. 3). However, eight and seven HTS Otus with relative abundance of > 1% in HZ and YC, respectively, were undetected in clone libraries and are relatively set apart from those with the rare Otus of < 1% (42 and 59 for HZ and YC, respectively).

### HTS profiling population-level dynamics of *Accumulibacter* in laboratory bioreactors

As shown in Fig. 4(a), the AS for seeding the bioreactor R' contained < 1% *Accumulibacter* in the total bacteria. The original AS and subsequent samples from this bioreactor exhibited dominant type II populations. After enrichment for only 7 days, the genus increased to 4.3% in total bacterial community, thereby suggesting a rapid growing response to

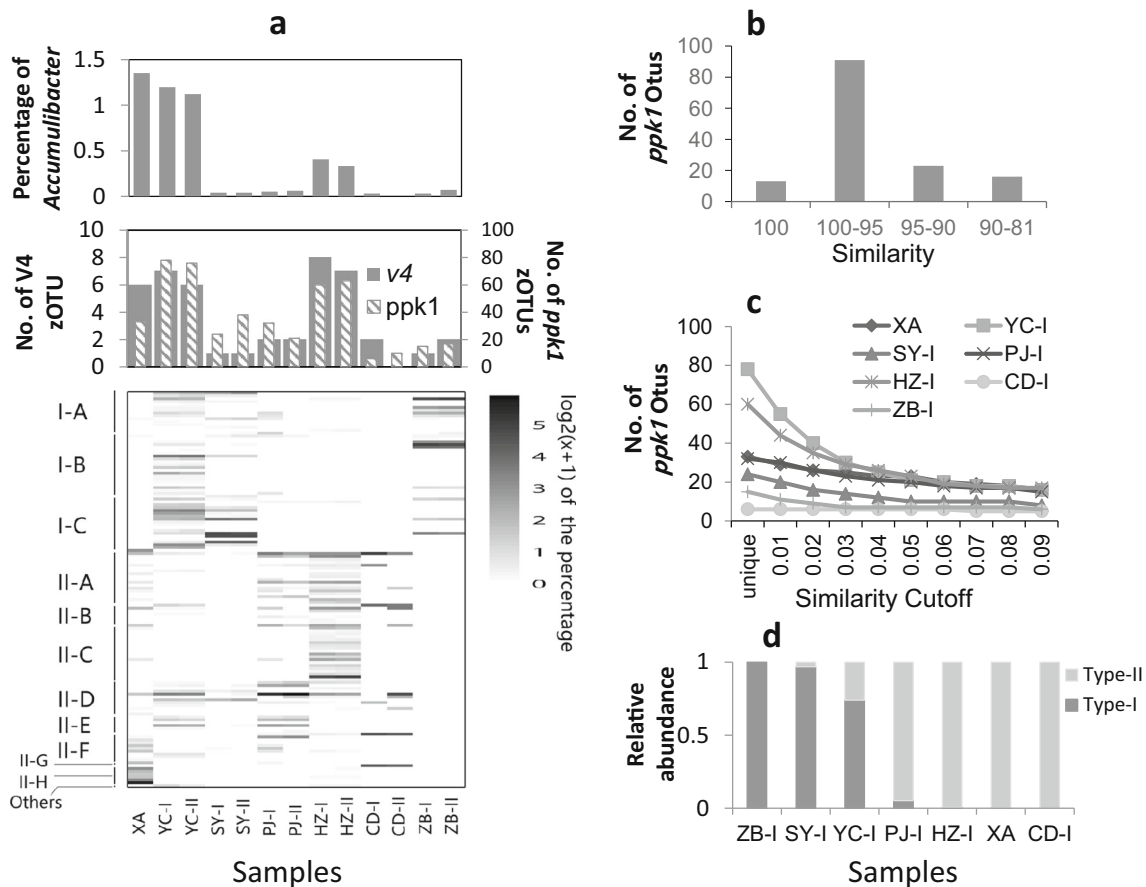


**Fig. 2** Population-level diversity of *Accumulibacter* in seven AS samples. (a) Relative abundance, number of V4 and *ppk1* Otus, and distribution of diverse *Accumulibacter* populations in the samples. (b) Distribution of similarity between *ppk1* Otus and references. (c) Number of clustered Otus at different similarity cut-offs for the *ppk1*

sequences that were detected in each sample. (d) Relative abundance of types I and II populations. Percentage data to generate the heatmap in panel A were transformed as  $\log_2(x + 1)$ , where  $x$  is the relative abundance of certain Otu to total *Accumulibacter*

the cultivation condition. However, the percentages kept at 3–4% until 29 days and then increased to 7% in day 36. Although the *Accumulibacter* percentage was relatively stable within 7–29 days, the population-level community structure significantly changed (Fig. 4(a)). The changes among populations within the same clade were unexpected. Otu4 that was affiliated with clade II-C gradually increased with the enriching period, whereas the other clade II-C population, that is, Otu8, decreased during the same period. Meanwhile, the three clade II-F populations, namely Otu21, Otu17, and Otu33, displayed increased and decreased relative stability from day 14 to day 36. In addition to the intraclade variations, the two Otus of clades II-A continuously increased during the enriching period. A dominant population in the original AS belonged to clade II-H, which is a recently proposed clade that has not been reported in previous studies on laboratory enrichment (Mao et al. 2015; Zhang et al. 2016). However, this population decreased rapidly in the laboratory system and reached an undetectable level at day 36. Our results suggested that this clade seemed uniquely present in the full-scale WWTPs. The extinction of this clade in the enrichment

systems may be due to the missing essential factors or to the unsuitable conditions.

Compared with the initial enrichment above, the dynamics of *Accumulibacter* populations in the long-term maintained MR from 730 days to 797 days were relatively simple (Fig. 4(b)). The top population shifted from a I-A strain to a II-F strain. Five bioreactors were inoculated from MR. There was a rapid loss of *Accumulibacter* due to the continuous aeration in R1, whereas the four other bioreactors that were inoculated from MR exhibited an overall similarity for most *Accumulibacter* populations (Fig. 4(c), (d)). Operational parameters verified the P removal deterioration in R1 and nitrification inhibition in R3 (Figure S4). R2 (control), R3 (no denitrification), and R4 (fed with acetate only) exhibited similar dynamic tendencies of the *Accumulibacter* populations. The process of denitrification had minimal effects on the *Accumulibacter* dynamics, because the difference between R2 and R3 was minimal. R5, which was fed with propionate as the sole C source, exhibited a much lower abundance of the two II-F populations (i.e., Otu2 and Otu9) and higher abundance of II-C (Otu4 and Otu5) than those in R2, R3, and R4. The variation of the major bacterial community in R1-

**Fig. 3** Comparison of *Accumulibacter* community structure as determined by clone library and HTS profiling for HZ and YC samples. All clone library sequences (31 each for HZ and YC) were listed after clustering at 99.5% similarity (allowing 1 mismatch) for their 254F-526R primer-free region. The HTS Otus corresponding to the clone sequences were determined by requiring > 99.5% similarity (allowing 1 mismatch) for the 235 nt primer-free region. The listed HTS Otus that were undetected in the clone library showed the relative abundance of total *Accumulibacter* of > 1%

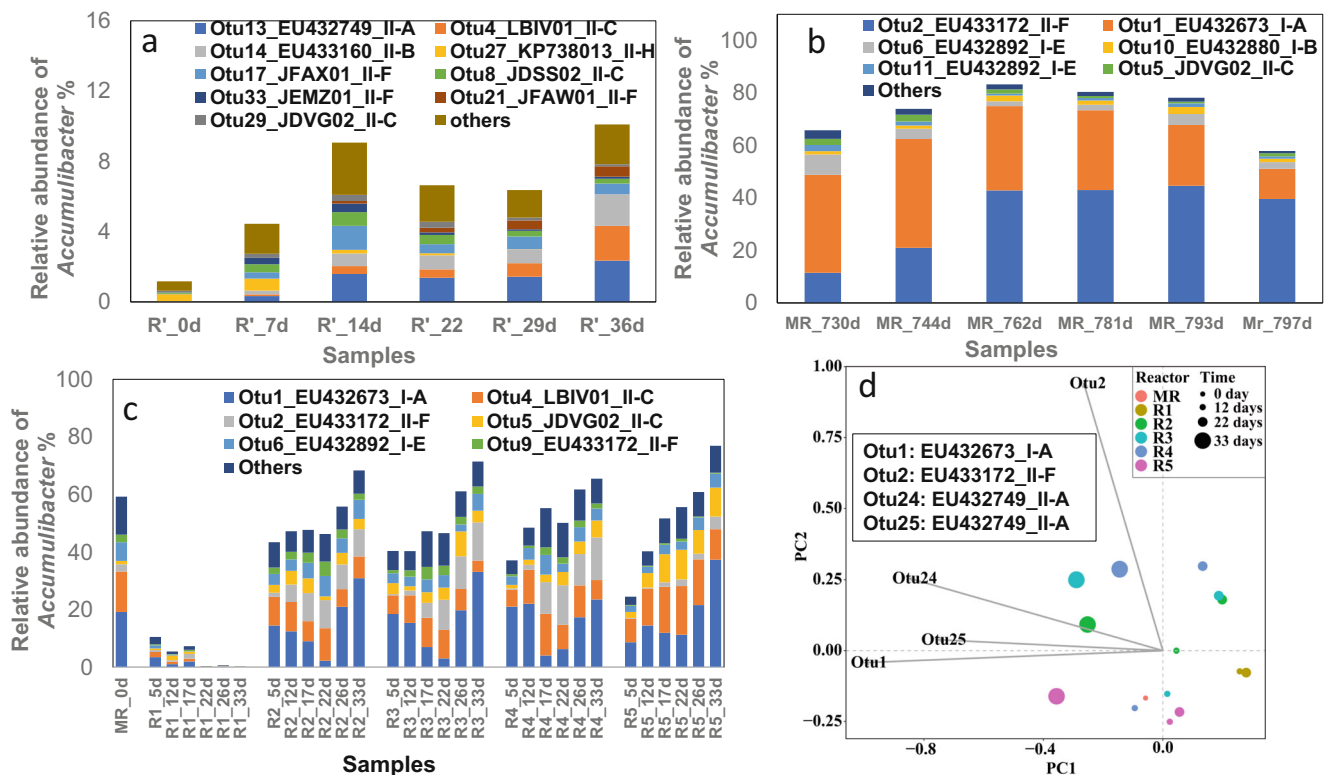
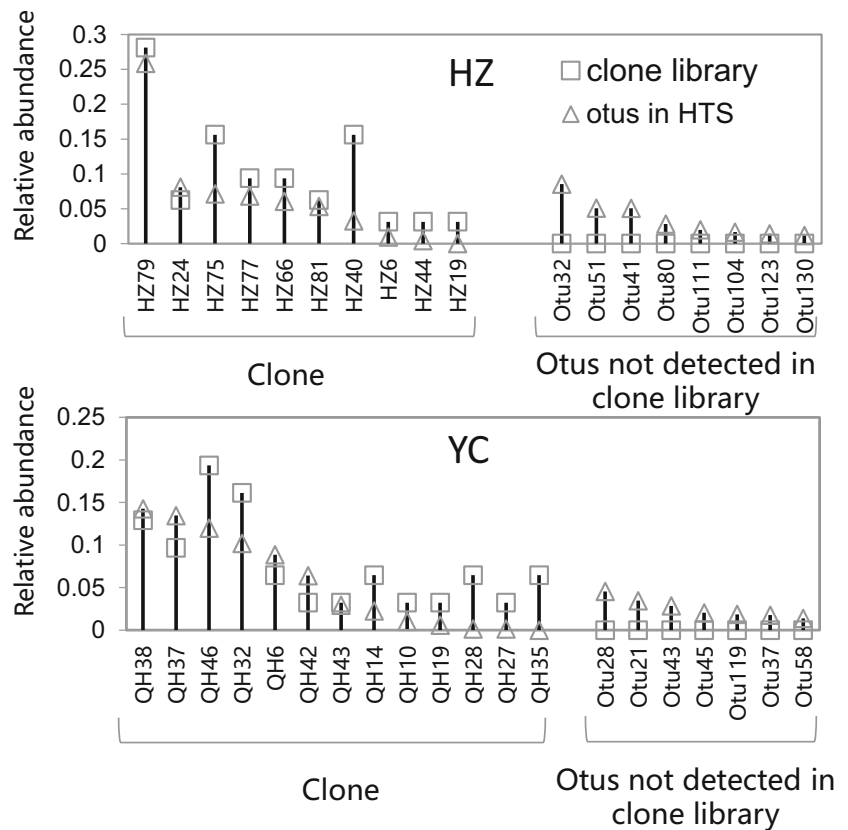


**Fig. 4** Population-level dynamics of *Accumulibacter* during laboratory reactor enrichment. Bioreactors including R' enriched from a seed AS from a full-scale WWTP (a), MR that was maintained in the laboratory for a long time (b) and five (R1–R5) under various conditions (c and d).

The biplot of the Unifrac distance-based principal component analysis was built for the samples collected at days 0, 12, 22, and 33 for the five bioreactors (d). The 33-day sample of R1 was excluded because the *Accumulibacter* that was detected in the V4 dataset was extremely low

R5 is also listed in Table S2 and Figure S5, which showed that *Plasticicumulans*-related taxa rapidly outcompeted *Accumulibacter* in R1.

PCA for V4 and *ppk1* datasets displayed a non-unidirectional dynamic of the bacterial community and *Accumulibacter* populations, respectively (Figs. 4(d) and S4). Along with the overall similar development of *Accumulibacter* diversity in R2, R3, and R4 bioreactors, the dynamics of *Accumulibacter* populations can be at least partially governed by biotic factors, such as the dynamics of other bacterial taxa. Given that the analytic pipeline of this study provided a conventional quantification of each *Accumulibacter* population (according to V4 and *ppk1* data) and other taxa (according to V4 data), we determined the co-occurrence pattern between *Accumulibacter* populations and the other bacteria based on their relative abundances.

### Co-occurrence analysis for *Accumulibacter* populations within bacterial community

Considering that unrelated samples compromise the robustness of network analysis, we performed the network analysis based on 37 datasets that were all derived from the MR or MR-derived R1–R5. The V4 Otus that were annotated as *Accumulibacter* were removed from the V4 Otu table and then merged with the *ppk1* Otu table. The Otus with low frequency (detected in < 50% samples) and abundance (average of < 0.1% in total bacteria or *Accumulibacter* for V4 and *ppk1* Otu) were filtered out before calculation correlation efficiencies. As shown in Fig. 5(a), *Accumulibacter* populations were involved in two separated clusters. Cluster I only comprised five *Accumulibacter* populations (three from type I and two from type II), whereas cluster II contained eight type II *Accumulibacter* populations along with other bacterial taxa, such as the Otus annotated as *Plasticicumulans*, *Proteobacteria*, *Bacteroidetes*, and *Verrucomicrobia*. Intertype exclusivity was observed, but it was not strict. Three and two *Plasticicumulans*-related Otus exhibited positive and negative correlation with cluster II, respectively (Fig. 5(a), (b)). Further examination of their sequences indicated that the former three *Plasticicumulans*-related Otus were affiliated with the *Competibacter* lineage, which never exceeded 3% of the total bacterial community (Table S2), whereas the latter two dominating in the R1 samples were related to *Plasticicumulans* according to the phylogeny proposed by McIlroy et al. (2014, 2015). The lineages of *Cytophagaceae* and *Prostheobacter* exhibited a similar phenomenon in which the Otus of these taxa can positively and negatively co-occur with *Accumulibacter* cluster II (Fig. 5(a), (b)).

## Discussion

As an inexpensive approach, the HTS of *ppk1* undoubtedly provided a more comprehensive profile of *Accumulibacter*

diversity in samples than a clone library. The primer of 526R that was designed for HTS exhibited high coverage among known *Accumulibacter* clades and suitable population-level resolution. The 16S rRNA gene determined the percentage of the total *Accumulibacter*, which helped in the quantification of each population's relative abundance. rRNA-based quantification cannot reflect the exact cell number percentages without reliable copy number correction of each Otus. However, considering that most Otus cannot be accurately annotated at the species level in the rrnDB (Stoddard et al. 2014), corrections were not performed in the present study.

To our knowledge, all previous qPCR-based studies that used clade-specific primers targeting *ppk1* to quantify the certain clades did not cover all recognized 14 clades (Camejo et al. 2016; Mao et al. 2015; Zhang et al. 2016) and the potential biases introduced by primer coverage, undefined cross-talking, and the presence of unrecognized clades. Generally, at most tens of *ppk1* representatives can be obtained from natural systems and full-scale or laboratory-scale samples through clone libraries (Mao et al. 2015; Peterson et al. 2008; Watson et al. 2019). However, our results suggested that methodological limitation can be a key to understanding the population-level diversity of *Accumulibacter*, especially intraclade variation. The clade-level diversity of *Accumulibacter* should be higher than the currently designated catalogs (14 clades in total) because of the presence of the remotely related sequences. Several sequences were incorrectly removed due to their rareness and low similarities when following the analytic pipeline.

Despite that high population-level diversity was observed in all full-scale AS samples, the exclusive distribution manner of type-level populations strongly suggested the niche differentiation of the two types. This phenomenon was further partially supported by our co-occurrence analysis. The metabolic features of the two types have been proposed as denitrification capability and adaptation on different phosphate concentrations (Acevedo et al. 2012; Flowers et al. 2009; Nurmiyanto et al. 2017; Welles et al. 2016). However, the evidence of full denitrification capability by using nitrate as the electron acceptor for type I *Accumulibacter* has been challenged experimentally and genomically, except for a special case of I-C under microaerobic conditions (Camejo et al. 2019; Rubio-Rincón et al. 2017; Skennerton et al. 2015). The WWTPs involved in this study were also treated with common municipal sewage, with relatively low phosphate concentration (commonly < 10 mg L<sup>-1</sup> in the influent). Thus, other unknown niches can play important roles in the distribution of *Accumulibacter* types I and II.

Continuous aeration can deteriorate EBPR activity and significantly decrease *Accumulibacter* (Ahn et al. 2007; Pijuan et al. 2006), although the P removal by *Accumulibacter* independent of the anaerobic phase, was supported by a subsequent study



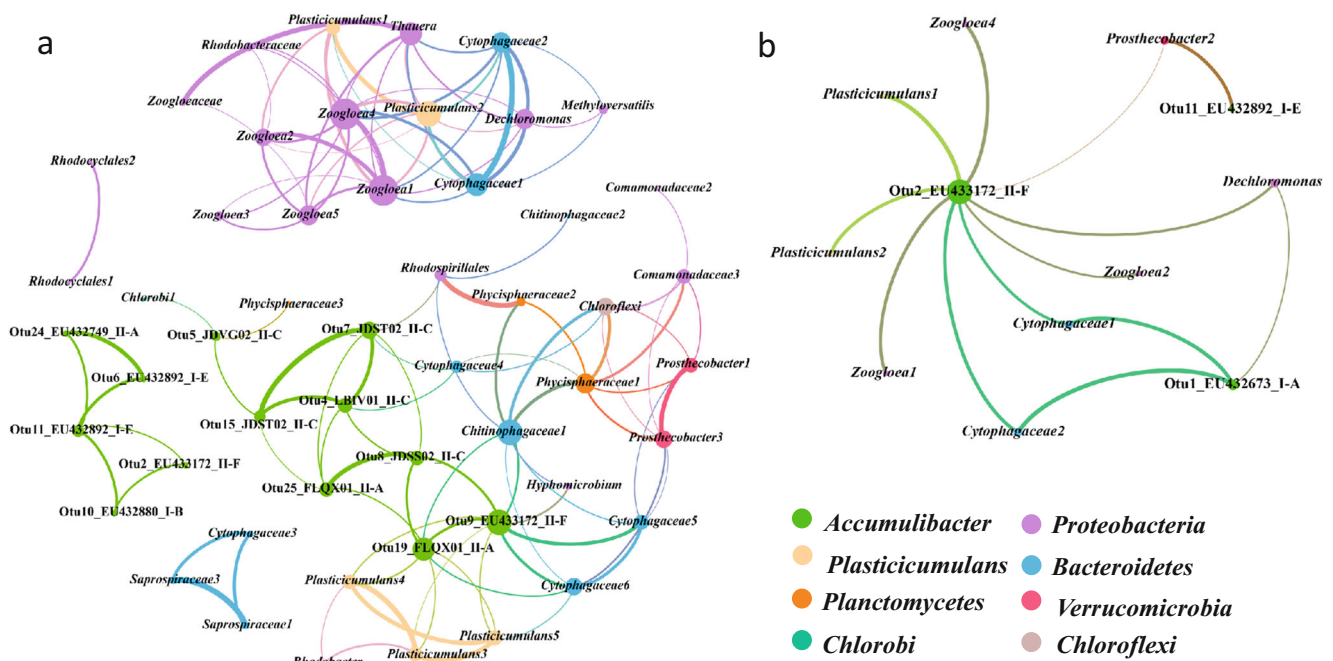


**Fig. 5** Co-occurrence (a) and negative correlation (b) between *Accumulibacter* populations and other bacterial taxa. The *ppk1* Otu of *Accumulibacter* and V4 Otus were affiliated with *Plasticicumulans*-related lineage, and six phyla were present as the nodes with different colors. The average abundance of all analyzed Otus were > 0.1% across all 37 samples on average, including seven from MR and 30 from R1–R5

(Nittami et al. 2011). Our results indicated that the deterioration of EBPR activity in our experimental systems can be due to the blooming of *Plasticicumulans*-related taxa. *Plasticicumulans*-related taxa are nontypical glycogen accumulating organism (GAOs) only detected in aerobic systems (McIlroy et al. 2014; McIlroy et al. 2015). Our results essentially supported the aerobic lifestyle of this lineage. The C source preference between acetate and propionate is clade specific. Our result was consistent with the fact that clade II-C seemed to have priority on propionate and metabolic flexibility compared with other clades (Nittami et al. 2017; Welles et al. 2017). Moreover, the *Accumulibacter* populations were insensitive to the block of nitrification–denitrification process, which in turn supported the fact that the denitrification contribution of PAOs is insignificant in common EBPR systems (Camejo et al. 2019; Rubio-Rincón et al. 2017; Zhao et al. 2019).

The co-occurrence and dynamic variation of the closely related taxa are ecological adapted to change the environments (Brazelton et al. 2010; Chafee et al. 2018). Unlike most natural systems with dramatically and continuously changed physiochemical conditions, laboratory EBPR bioreactors were relatively stable under macroscale. However, the dynamics of *Accumulibacter* populations can be partially attributed to the microscale environment change, which was introduced by the activities of overall microbial community. Few bacterial taxa that exhibited co-occurring pattern with *Accumulibacter* were discovered by the proposed quantitative pipeline. These results can be

explained by either niche co-selection or microbial interactions. Therefore, *Cytophagaceae* is occasionally reported in *Accumulibacter* dominant bioreactors (Church et al. 2018; Law et al. 2016). Its functions have not been characterized beside that it seemed related to aeration condition (Law et al. 2016). One potential explanation can be the environmental co-selective or reverse-selective effect that caused its co-occurrence or negative correlation with *Accumulibacter* in our dataset, instead of direct interaction among microorganisms. However, strains from *Prostheco bacter* in *Verrucomicrobia* have been extensively detected with subdominant abundance in diverse laboratory EBPR systems, thereby indicating their specific adaptation to a unique niche (Gao et al. 2019; Garcia Martin et al. 2006; Lawson et al. 2015; Li et al. 2016). The roles that these strains played in the system included GAO, PAO, and/or unknown functions that require further investigation. Moreover, the widely investigated *Competibacter*-related GAOs were previously believed to be strict competitors of *Accumulibacter* (Oehmen et al. 2007). A recent study proposed that *Competibacter*-related GAOs can cooperate with *Accumulibacter* to realize simultaneous N and P removal in bioreactors (Rubio-Rincón et al. 2017). Together with our result that the subdominant *Competibacter*-related lineage can statistically co-occur with *Accumulibacter* populations, our findings increased interest in the examination of their metabolic relationships rather than competition.

In conclusion, our study introduced a convenient pipeline to profile the population-level diversity and dynamics of

*Accumulibacter* in the community. Its advantages lie in profiling microdiversity of *Accumulibacter* beyond the clade level and provide a quantitative profile of each *Accumulibacter* population and other microorganisms that can co-occur and metabolically interact with *Accumulibacter*. A detailed information of the precise functional specificity and niche differentiation in diverse *Accumulibacter* strains may be achieved by applying the approach to a wide variety of AS samples from full-scale WWTPs or laboratory reactors. The pipeline can be transplanted for other key functional microorganisms in natural and artificial systems.

**Acknowledgments** Prof. Xin Yu and Mr. Chengsong Ye are thanked for providing the activated sludge samples from WWTPs. Mr. Le Yang is thanked for his helps in operating partial bioreactors.

**Funding information** The authors received financial supports from the National Natural Science Foundation of China (No. 31500100 and No. 31670492).

**Data availability** The *ppk1* sequences generated from clone libraries were deposited in GenBank under the accession no. MK818549–MK818571. The high throughput data are available at the NCBI Sequence Read Archive database under the accession no. PRJNA543374.

## Compliance with ethical standards

**Conflict of interest** The authors declare that they have no conflicts of interest.

**Ethical approval** This article does not contain any studies with human participants or animals performed by any of the authors.

## References

- Acevedo B, Oehmen A, Carvalho G, Seco A, Borrás L, Barat R (2012) Metabolic shift of polyphosphate-accumulating organisms with different levels of polyphosphate storage. *Water Res* 46(6):1889–1900. <https://doi.org/10.1016/j.watres.2012.01.003>
- Ahn J, Schroeder S, Beer M, McLroy S, Bayly RC, May JW, Vasiliadis G, Seviour RJ (2007) Ecology of the microbial community removing phosphate from wastewater under continuously aerobic conditions in a sequencing batch reactor. *Appl Environ Microbiol* 73(7):2257–2270. <https://doi.org/10.1128/AEM.02080-06>
- Albertsen M, Hansen LB, Saunders AM, Nielsen PH, Nielsen KL (2012) A metagenome of a full-scale microbial community carrying out enhanced biological phosphorus removal. *ISME J* 6(6):1094–1106. <https://doi.org/10.1038/ismej.2011.176>
- Albertsen M, McLroy SJ, Stokholm-Bjerregaard M, Karst SM, Nielsen PH (2016) “*Candidatus* Propionivibrio aalborgensis”: a novel glycogen accumulating organism abundant in full-scale enhanced biological phosphorus removal plants. *Front Microbiol* 7(119)
- APHA (1998) Standard methods for the examination of water and wastewater. American Public Health Association, Washington D.C
- Barr JJ, Dutilh BE, Skennerton CT, Fukushima T, Hastie ML, Gorman JJ, Tyson GW, Bond PL (2016) Metagenomic and metaproteomic analyses of *Accumulibacter* phosphatis-enriched floccular and granular biofilm. *Environ Microbiol* 18(1):273–287. <https://doi.org/10.1111/1462-2920.13019>
- Bastian M, Heymann S, Jacomy M (2009) Gephi: an open source software for exploring and manipulating networks. In: international conference on weblogs and social media
- Brazelton WJ, Sogin ML, Baross JA (2010) Multiple scales of diversification within natural populations of archaea in hydrothermal chimney biofilms. *Environ Microbiol Rep* 2(2):236–242. <https://doi.org/10.1111/j.1758-2229.2009.00097.x>
- Camejo PY, Owen BR, Martirano J, Ma J, Kapoor V, Santo Domingo J, McMahon KD, Noguera DR (2016) *Candidatus* *Accumulibacter* phosphatis clades enriched under cyclic anaerobic and microaerobic conditions simultaneously use different electron acceptors. *Water Res* 102:125–137. <https://doi.org/10.1016/j.watres.2016.06.033>
- Camejo PY, Oyserman BO, McMahon KD, Noguera DR (2019) Integrated omic analyses provide evidence that a “*Candidatus* *Accumulibacter* phosphatis” strain performs denitrification under microaerobic conditions. *BioRxiv* 4(1)
- Chafee M, Fernández-Guerra A, Buttigieg PL, Gerdtts G, Eren AM, Teeling H, Amann RI (2018) Recurrent patterns of microdiversity in a temperate coastal marine environment. *ISME J* 12(1):237–252. <https://doi.org/10.1038/ismej.2017.165>
- Church J, Ryu H, Sadmani AA, Randall AA, Santo Domingo J, Lee WH (2018) Multiscale investigation of a symbiotic microalgal-integrated fixed film activated sludge (MAIFAS) process for nutrient removal and photo-oxygenation. *Bioresour Technol* 268:128–138. <https://doi.org/10.1016/j.biortech.2018.07.123>
- Edgar RC (2010) Search and clustering orders of magnitude faster than BLAST. *Bioinformatics* 26(19):2460–2461. <https://doi.org/10.1093/bioinformatics/btq461>
- Edgar RC (2016a) UCHIME2: improved chimera prediction for amplicon sequencing. *BioRxiv* 074252. <https://doi.org/10.1101/074252>
- Edgar RC (2016b) UNOISE2: improved error-correction for Illumina 16S and ITS amplicon sequencing. *BioRxiv* 081257. <https://doi.org/10.1101/081257>
- Edgar RC (2018) UNCROSS2: identification of cross-talk in 16S rRNA OTU tables. *BioRxiv* 400762. <https://doi.org/10.1101/400762>
- Flowers JJ, He SM, Yilmaz S, Noguera DR, McMahon KD (2009) Denitrification capabilities of two biological phosphorus removal sludges dominated by different ‘*Candidatus* *Accumulibacter*’ clades. *Environ Microbiol Rep* 1(6):583–588. <https://doi.org/10.1111/j.1758-2229.2009.00090.x>
- Gao H, Mao Y, Zhao X, Liu W-T, Zhang T, Wells G (2019) Genome-centric metagenomics resolves microbial diversity and prevalent truncated denitrification pathways in a denitrifying PAO-enriched bioprocess. *Water Res* 155:275–287. <https://doi.org/10.1016/j.watres.2019.02.020>
- Garcia Martin H, Ivanova N, Kunin V, Wamecke F, Barry KW, McHardy AC, Yeates C, He S, Salamov AA, Szeto E, Dalin E, Putnam NH, Shapiro HJ, Pangilinan JL, Rigoutsos I, Kyrpides NC, Blackall LL, McMahon KD, Hugenholtz P (2006) Metagenomic analysis of two enhanced biological phosphorus removal (EBPR) sludge communities. *Nat Biotechnol* 24(10):1263–1269. <https://doi.org/10.1038/nbt1247>
- Gruber-Dominger C, Pester M, Kitzinger K, Savio DF, Loy A, Rattei T, Wagner M, Daims H (2015) Functionally relevant diversity of closely related *Nitrospira* in activated sludge. *ISME J* 9(3):643–655. <https://doi.org/10.1038/ismej.2014.156>
- He S, Gall DL, McMahon KD (2007) “*Candidatus* *Accumulibacter*” population structure in enhanced biological phosphorus removal sludges as revealed by polyphosphate kinase genes. *Appl Environ Microbiol* 73(18):5865–5874. <https://doi.org/10.1128/AEM.01207-07>
- Ju F, Zhang T (2015) Bacterial assembly and temporal dynamics in activated sludge of a full-scale municipal wastewater treatment plant. *ISME J* 9(3):683–695. <https://doi.org/10.1038/ismej.2014.162>
- Kip N, Dutilh BE, Pan Y, Bodrossy L, Neveling K, Kwint MP, Jetten MS, Op den Camp HJ (2011) Ultra-deep pyrosequencing of *pmoA*

- amplicons confirms the prevalence of *Methylomonas* and *Methylocystis* in *Sphagnum* mosses from a Dutch peat bog. *Environ Microbiol Rep* 3(6):667–673. <https://doi.org/10.1111/j.1758-2229.2011.00260.x>
- Kozich JJ, Westcott SL, Baxter NT, Highlander SK, Schloss PD (2013) Development of a dual-index sequencing strategy and curation pipeline for analyzing amplicon sequence data on the MiSeq Illumina sequencing platform. *Appl Environ Microbiol* 79(17):5112–5120. <https://doi.org/10.1128/AEM.01043-13>
- Kumar S, Stecher G, Tamura K (2016) MEGA7: molecular evolutionary genetics analysis version 7.0 for bigger datasets. *Mol Biol Evol* 33(7):1870–1874. <https://doi.org/10.1093/molbev/msw054>
- Law Y, Kirkegaard RH, Cokro AA, Liu X, Arumugam K, Xie C, Stokholm-Bjerregaard M, Drautz-Moses DI, Nielsen PH, Wuertz S (2016) Integrative microbial community analysis reveals full-scale enhanced biological phosphorus removal under tropical conditions. *Sci Rep* 6:25719. <https://doi.org/10.1038/srep25719>
- Lawson CE, Strachan BJ, Hanson NW, Hahn AS, Hall ER, Rabinowitz B, Mavinic DS, Ramey WD, Hallam SJ (2015) Rare taxa have potential to make metabolic contributions in enhanced biological phosphorus removal ecosystems. *Environ Microbiol* 17(12):4979–4993. <https://doi.org/10.1111/1462-2920.12875>
- Li D, Lv Y, Zeng H, Zhang J (2016) Long term operation of continuous-flow system with enhanced biological phosphorus removal granules at different COD loading. *Bioresour Technol* 216:761–767. <https://doi.org/10.1016/j.biortech.2016.06.022>
- Li C, Zeng W, Li N, Guo Y, Peng Y (2019) Population structure and morphotype analysis of “*Candidatus Accumulibacter*” through FISH-Staining-Flow cytometry. *Appl Environ Microbiol* 02943:18. <https://doi.org/10.1128/AEM.02943-18>
- MacConaill LE, Burns RT, Nag A, Coleman HA, Slevin MK, Giorda K, Light M, Lai K, Jarosz M, McNeill MS, Ducar MD, Meyerson M, Thomer AR (2018) Unique, dual-indexed sequencing adapters with UMIs effectively eliminate index crosstalk and significantly improve sensitivity of massively parallel sequencing. *BMC Genomics* 19(1):30
- Mao Y, Yu K, Xia Y, Chao Y, Zhang T (2014) Genome reconstruction and gene expression of “*Candidatus Accumulibacter phosphatis*” Clade IB performing biological phosphorus removal. *Environ Sci Technol* 48(17):10363–10371. <https://doi.org/10.1021/es502642b>
- Mao Y, Graham DW, Tamaki H, Zhang T (2015) Dominant and novel clades of *Candidatus Accumulibacter phosphatis* in 18 globally distributed full-scale wastewater treatment plants. *Sci Rep* 5:11857. <https://doi.org/10.1038/srep11857>
- McIlroy SJ, Albertsen M, Andresen EK, Saunders AM, Kristiansen R, Stokholm-Bjerregaard M, Nielsen KL, Nielsen PH (2014) ‘*Candidatus Competibacter*’-lineage genomes retrieved from metagenomes reveal functional metabolic diversity. *ISME J* 8(3):613–624. <https://doi.org/10.1038/ismej.2013.162>
- McIlroy SJ, Nittami T, Kanai E, Fukuda J, Saunders AM, Nielsen PH (2015) Re-appraisal of the phylogeny and fluorescence in situ hybridization probes for the analysis of the *Competibacteraceae* in wastewater treatment systems. *Environ Microbiol Rep* 7(2):166–174. <https://doi.org/10.1111/1758-2229.12215>
- McMurdie PJ, Holmes S (2013) phyloseq: an R package for reproducible interactive analysis and graphics of microbiome census data. *PLoS One* 8(4):e61217. <https://doi.org/10.1371/journal.pone.0061217>
- Nancharaiyah Y, Mohan SV, Lens P (2016) Recent advances in nutrient removal and recovery in biological and bioelectrochemical systems. *Bioresour Technol* 215:173–185. <https://doi.org/10.1016/j.biortech.2016.03.129>
- Nittami T, Oi H, Matsumoto K, Seviour RJ (2011) Influence of temperature, pH and dissolved oxygen concentration on enhanced biological phosphorus removal under strictly aerobic conditions. *New Biotechnol* 29(1):2–8. <https://doi.org/10.1016/j.nbt.2011.06.012>
- Nittami T, Mukai M, Uematsu K, Yoon LW, Schroeder S, Chua ASM, Fukuda J, Fujita M, Seviour RJ (2017) Effects of different carbon sources on enhanced biological phosphorus removal and “*Candidatus Accumulibacter*” community composition under continuous aerobic condition. *Appl Microbiol Biotechnol* 101(23–24):8607–8619. <https://doi.org/10.1007/s00253-017-8571-3>
- Nurmiyanto A, Kodera H, Kindaichi T, Ozaki N, Aoi Y, Ohashi A (2017) Dominant *Candidatus Accumulibacter phosphatis* enriched in response to phosphate concentrations in EBPR process. *Microbes Environ* 32(3):260–267. <https://doi.org/10.1264/jsme2.ME17020>
- Oehmen A, Lemos PC, Carvalho G, Yuan Z, Keller J, Blackall LL, Reis MA (2007) Advances in enhanced biological phosphorus removal: from micro to macro scale. *Water Res* 41(11):2271–2300. <https://doi.org/10.1016/j.watres.2007.02.030>
- Ong YH, Chua AS, Lee BP, Ngoh GC (2013) Long-term performance evaluation of EBPR process in tropical climate: start-up, process stability, and the effect of operational pH and influent C:P ratio. *Water Sci Technol* 67(2):340–346. <https://doi.org/10.2166/wst.2012.552>
- Oyserman BO, Noguera DR, del Rio TG, Tringe SG, McMahon KD (2016) Metatranscriptomic insights on gene expression and regulatory controls in *Candidatus Accumulibacter phosphatis*. *ISME J* 10(4):810–822. <https://doi.org/10.1038/ismej.2015.155>
- Peterson SB, Warnecke F, Madejska J, McMahon KD, Hugenholtz P (2008) Environmental distribution and population biology of *Candidatus Accumulibacter*, a primary agent of biological phosphorus removal. *Environ Microbiol* 10(10):2692–2703. <https://doi.org/10.1111/j.1462-2920.2008.01690.x>
- Pijuan M, Guisasaola A, Baeza JA, Carrera J, Casas C, Lafuente J (2006) Net P-removal deterioration in enriched PAO sludge subjected to permanent aerobic conditions. *J Biotechnol* 123(1):117–126. <https://doi.org/10.1016/j.jbiotec.2005.10.018>
- Remmas N, Melidis P, Katsioui E, Ntougias S (2016) Effects of high organic load on *amoA* and *nirS* gene diversity of an intermittently aerated and fed membrane bioreactor treating landfill leachate. *Bioresour Technol* 220:557–565. <https://doi.org/10.1016/j.biortech.2016.09.009>
- Rubio-Rincón F, Lopez-Vazquez C, Welles L, van Loosdrecht M, Brdjanovic D (2017) Cooperation between *Candidatus Competibacter* and *Candidatus Accumulibacter* clade I, in denitrification and phosphate removal processes. *Water Res* 120:156–164. <https://doi.org/10.1016/j.watres.2017.05.001>
- Saad SA, Welles L, Abbas B, Lopez-Vazquez CM, van Loosdrecht MCM, Brdjanovic D (2016) Denitrification of nitrate and nitrite by ‘*Candidatus Accumulibacter phosphatis*’ clade IC. *Water Res* 105:97–109. <https://doi.org/10.1016/j.watres.2016.08.061>
- Skenneron CT, Barr JJ, Slater FR, Bond PL, Tyson GW (2015) Expanding our view of genomic diversity in *Candidatus Accumulibacter* clades. *Environ Microbiol* 17(5):1574–1585. <https://doi.org/10.1111/1462-2920.12582>
- Slater FR, Johnson CR, Blackall LL, Beiko RG, Bond PL (2010) Monitoring associations between clade-level variation, overall community structure and ecosystem function in enhanced biological phosphorus removal (EBPR) systems using terminal-restriction fragment length polymorphism (T-RFLP). *Water Res* 44(17):4908–4923. <https://doi.org/10.1016/j.watres.2010.07.028>
- Stoddard SF, Smith BJ, Hein R, Roller BR, Schmidt TM (2014) rmDB: improved tools for interpreting rRNA gene abundance in bacteria and archaea and a new foundation for future development. *Nucleic Acids Res* 43(D1):D593–D598. <https://doi.org/10.1093/nar/gku1201>
- Vargas M, Casas C, Baeza J (2009) Maintenance of phosphorus removal in an EBPR system under permanent aerobic conditions using propionate. *Biochem Eng J* 43(3):288–296. <https://doi.org/10.1016/j.bej.2008.10.013>

- Varghese NJ, Mukherjee S, Ivanova N, Konstantinidis KT, Mavrommatis K, Kyrpides NC, Pati A (2015) Microbial species delineation using whole genome sequences. *Nucleic Acids Res* 43(14):6761–6771. <https://doi.org/10.1093/nar/gkv657>
- Watson S, Needoba J, Peterson T (2019) Widespread detection of *Candidatus Accumulibacter phosphatis*, a polyphosphate-accumulating organism, in sediments of the Columbia River estuary. *Environ Microbiol Rep* 21(4):1369–1382. <https://doi.org/10.1111/1462-2920.14576>
- Welles L, Lopez-Vazquez CM, Hooijmans CM, van Loosdrecht MCM, Brdjanovic D (2016) Prevalence of ‘*Candidatus Accumulibacter phosphatis*’ type II under phosphate limiting conditions. *AMB Express* 6(1):44. <https://doi.org/10.1186/s13568-016-0214-z>
- Welles L, Abbas B, Sorokin DY, Lopez-Vazquez CM, Hooijmans CM, van Loosdrecht M, Brdjanovic D (2017) Metabolic response of “*Candidatus Accumulibacter Phosphatis*” Clade II C to changes in influent P/C ratio. *Front Microbiol* 7:2121. <https://doi.org/10.3389/fmicb.2016.02121>
- Yoon SH, Ha SM, Kwon S, Lim J, Kim Y, Seo H, Chun J (2017) Introducing EzBioCloud: a taxonomically united database of 16S rRNA gene sequences and whole-genome assemblies. *Int J Syst Evol Microbiol* 67(5):1613–1617. <https://doi.org/10.1099/ijsem.0.001755>
- Zhang T, Shao MF, Ye L (2012) 454 Pyrosequencing reveals bacterial diversity of activated sludge from 14 sewage treatment plants. *ISME J* 6(6):1137–1147. <https://doi.org/10.1038/ismej.2011.188>
- Zhang AN, Mao Y, Zhang T (2016) Development of quantitative real-time PCR assays for different clades of “*Candidatus Accumulibacter*”. *Sci Rep* 6:23993. <https://doi.org/10.1038/srep23993>
- Zhao J, Wang X, Li X, Jia S, Wang Q, Peng Y (2019) Improvement of partial nitrification endogenous denitrification and phosphorus removal system: balancing competition between phosphorus and glycogen accumulating organisms to enhance nitrogen removal without initiating phosphorus removal deterioration. *Bioresour Technol* 281:382–391. <https://doi.org/10.1016/j.biortech.2019.02.109>

**Publisher's note** Springer Nature remains neutral with regard to jurisdictional claims in published maps and institutional affiliations.